Hilo, A. K., Abu Talib, A. R., Acosta Iborra, A., Hameed Sultan, M. T. & Abdul Hamid, M. F. (2020). Effect of corrugated wall combined with backward-facing step channel on fluid flow and heat transfer. *Energy*, vol. 190, 116294.

DOI: 10.1016/j.energy.2019.116294

Effect of Corrugated Wall Combined with Backward-Facing Step Channel on Fluid Flow and Heat Transfer

Ali Kareem Hilo[1], Abd Rahim Abu Talib[1,2], Antonio Acosta Iborra[3], Mohammed Thariq Hameed Sultan[2], Mohd Faisal Abdul Hamid[1,2]*

[1]*Aerodynamic, Heat Transfer and Propulsion Group, Department of Aerospace Engineering, Faculty of Engineering, Universiti Putra Malaysia, 43400 Serdang, Selangor, Malaysia*

[2]*Aerospace Malaysia Research Centre, Faculty of Engineering, Universiti Putra Malaysia, 43400 Serdang, Selangor, Malaysia*

[3]*Department of Thermal and Fluids Engineering, Carlos III University of Madrid, Avda. de la Universidad 30, 28911 Leganés, Madrid, Spain*

[*]Corresponding author email: abdrahim@upm.edu.my

Abstract

The turbulent fluid flow and heat transfer were numerically studied through backward-facing step combined with various corrugated walls. The governing equation was solved using Finite Volume Method (FVM) and the SIMPLE algorithm was applied to investigate the effect of backward-facing step with corrugated downstream on heat transfer characteristics. A constant heat flux was applied on the downstream wall, while the other walls were considered as adiabatic surfaces. Parameters such as corrugated design, amplitude height (1, 2, 3, 4 and 5 mm) and Reynolds number (*Re*) in the range of 5,000 to 20,000 were used. The performance evaluation criteria were estimated to show the heat transfer augmentation. The results indicated that using a corrugated wall with a backward-facing step increased significantly the heat transfer accompanied by a slight increase in skin friction coefficient simultaneously. The best heat transfer augmentation was observed for the trapezoidal corrugation at 4 mm amplitude height and 20 mm pitch diameter. Combining the corrugated wall with backward-facing step enhanced the Nusselt number (*Nu*) up to 62% at *Re* = 5,000. The performance evaluation criteria increased with the increase of amplitude height until it reached 4 mm and then decreased steeply.

Keywords: Backward-facing step; Corrugated wall; Fluid flow; Heat transfer enhancement.

1.1 Introduction

The study of heat and mass transfer with separation and reattachment phenomena are commonly used in various engineering applications. The fluid flow and heat transfer through the backward-facing step is one of the interesting areas in several research studies. The backward-facing step has been used in different industrial heat transfer applications such as in combustors, gas turbine engines, aircraft, and buildings. Several studies have indicated that the separated flow has a significant influence on the thermal performance and heat transfer mechanism of heat exchanger [1]–[3]. The fluid and geometry parameter for improving the efficiency of heat transfer application has been investigated widely [4]–[10]. However, the majority of studies considered the isothermal flow, commonly in the smooth facing step channel.

A numerical study was performed by Abu-Nada [11] on the entropy through a two-dimensional backward-facing step for various expansion ratios such as 1/4, 1/3, 1/2, 2/3, and 3/4. The results demonstrated that as the Reynolds number (*Re*) increased, the value of the total entropy generation number also increased. For lower *Re*, as the expansion ratio (ER) increased the total entropy generation number decreased. Nie and Armaly [12] investigated the effect of step height of backward-facing step on laminar fluid flow and the heat transfer characteristic. They found that as the step height increased, the prime recirculation zone and the surface Nusselt number ($\overline{Nu}$) increased as well. Moreover, the maximum friction coefficient amplified as the step height increased in the prime recirculation zone. Armaly *et al*., [13] performed an experimental study to determine the velocity laminar flow over a backward-facing step by using two-component laser Doppler velocimeter.

Laminar forced convective flow through a backward-facing step placed in a duct was investigated by Al-aswadi *et al*., [14]. The duct expansion ratio was 2, and the step height was 4.8 mm. The *Re* values were kept in the range of 50 to 175. It was observed that the recirculation regime augmented as *Re* was increased. Togun *et al*., [15] studied the heat transfer of laminar and turbulent flow over a backward-facing step. The *Re* range was 5,000 to 20,000 for the turbulent range and 50 to 200 for the laminar range, and the expansion ratio was 2. The results showed that the expansion ratio had an effect on the increasing of *Nu* and that was accounted by the growth of recirculation regime downstream. Xue *et al*., [16][17] and Hsieh *et al*., [18] studied the fluid flow and heat transfer characteristics over micro-scale

backward-facing step. Moreover, many previous investigations have been reviewed by Mohammed *et al*., [19] in this study area and it was found that an increment of parameters, for instance, step height, fluid velocity, aspect ratio and Prandtl number (*Pr*) increased *Nu* and vice versa for the expansion ratio. Nonetheless, they did not focus on the augmentation of heat transfer in backward-facing step using turbulators, obstacles or protrusions.

It is worth to mention that a limited number of investigations have focused on the characteristic of fluid flow and heat transfer through backward-facing step with a corrugated bottom and one of them was carried out by Selimefendigil and Oztop [20]. Surface corrugation has been one of the techniques that were used to alter the flow and heat transfer characteristics in a variety of geometries in various thermal boundary conditions [21]–[27]. Ajeel *et al*., [28] investigated the thermal and hydraulic characteristics of turbulent nanofluid flow in different types of corrugated channel. The results showed that the trapezoidal channel had a higher effect on thermal performance compared with straight and zigzag channels. Abed *et al*., [29] investigated the effect of geometrical parameters (longitudinal pitch and wavy amplitudes) of the trapezoidal channel on the heat transfer and fluid flow under turbulent flow. The results showed that trapezoidal corrugated channel with 6 mm longitudinal pitch and 2.5 mm height were the best parameters for energy saving.

Ahmed *et al*., [30] investigated three various corrugated channels namely, straight, sinusoidal, and trapezoidal. Their results showed that the highest heat transfer improvement was obtained from trapezoidal channels compared to the sinusoidal channel and straight channel which obtained the lowest heat transfer rates. Navaei *et al*., [31] investigated the effects of different geometrical parameters on the thermal performance of rib grooved channels. Finite Volume Method (FVM) was applied to solve the governing equation under turbulent flow. The results showed that the highest *Nu* was at semi-circular with pitch 48 mm and height 8 mm. Eiamsa-ard *et al*., [32] studied the turbulent flow characteristics over periodic cavities in addition to thermal performances and flow frictional behaviours. The numerical results were computed using different models, namely the $k-\varepsilon$ standard, RNG $k-\omega$ model, and the SST $k-\omega$ model. The results indicated that the RNG $k-\varepsilon$ turbulent model was the best one to determine the characteristic of heat transfer and fluid flow over a periodic cavity channel.

Recently, Ajeel *et al*., [33] studied the effect of the geometrical parameter of the trapezoidal corrugated channel on heat transfer and fluid flow characteristics. To compute the turbulent flow, $k-\varepsilon$ turbulent model was applied. The results indicated that the height to width parameters had more effect on the heat transfer enhancement compared to the pitch to length parameters. Mohammed *et al*., [34] investigated the effects of four different types of vortex generator on transient laminar flow through a horizontal backward-facing step channel. The result showed that the front face triangular vortex generator had a greater value of performance evaluation criteria (PEC) and average *Nu* while the trapezoidal had the lowest value. Moreover, the triangular shape had the highest value of skin friction factor at the *Re* value of 150. Ahmed *et al*., [35] numerically studied the effect of laminar forced convection nanofluid on fluid flow and heat transfer through the micro backward-facing step channel with different types of turbulators. The results indicated that the case of rectangular wing turbulators at *Re* = 180 and attack angle 60° has the highest heat transfer accompanied with a slight increase in the pressure drop. The performance evaluation index increases as the *Re* increase until 180 and then a sharp decrease has been observed.

Based on previous literature, there are many studies which have been carried out to enhance heat transfer and flow. However, no study has investigated the case of combined backward-facing step with corrugated wall and come up with a novel combined channel. The main objective of this study was to investigate the turbulent flow and heat transfer over the backward-facing step channel combined with a different corrugated wall such as zigzag, triangular and trapezoidal. Numerical results have been obtained for *Re* in the range 5,000 to 20,000 step height = 10 mm, amplitude height = 1, 2, 3, 4 and 5 mm, pitch diameter = 20 mm, and the test section length = 200 mm.

1.2 Numerical implementations

1.2.1 Assumptions and physical model

The flow configuration and geometry used in this study is illustrated in **Fig.** 1. In order to ensure that the flow is fully developed in the channel, the upstream wall length was adjusted to 200 mm and the downstream wall length was 300 mm. The inlet and outlet high were10 mm and 20 mm respectively, with an expansion ratio of 2. **Fig.** (A) shows the smooth facing

step channel, and **Fig.** (B) and (C) show the triangular and trapezoidal facing step respectively. The pitch diameter (20 mm) and the amplitude height (1, 2, 3, 4, and 5 mm) of the channel are denoted by P and a respectively. A constant heat flux of 4 KW/m^2 over 200 mm was applied to the downstream wall, while the other walls were considered as adiabatic surfaces. The working fluid was pure water.

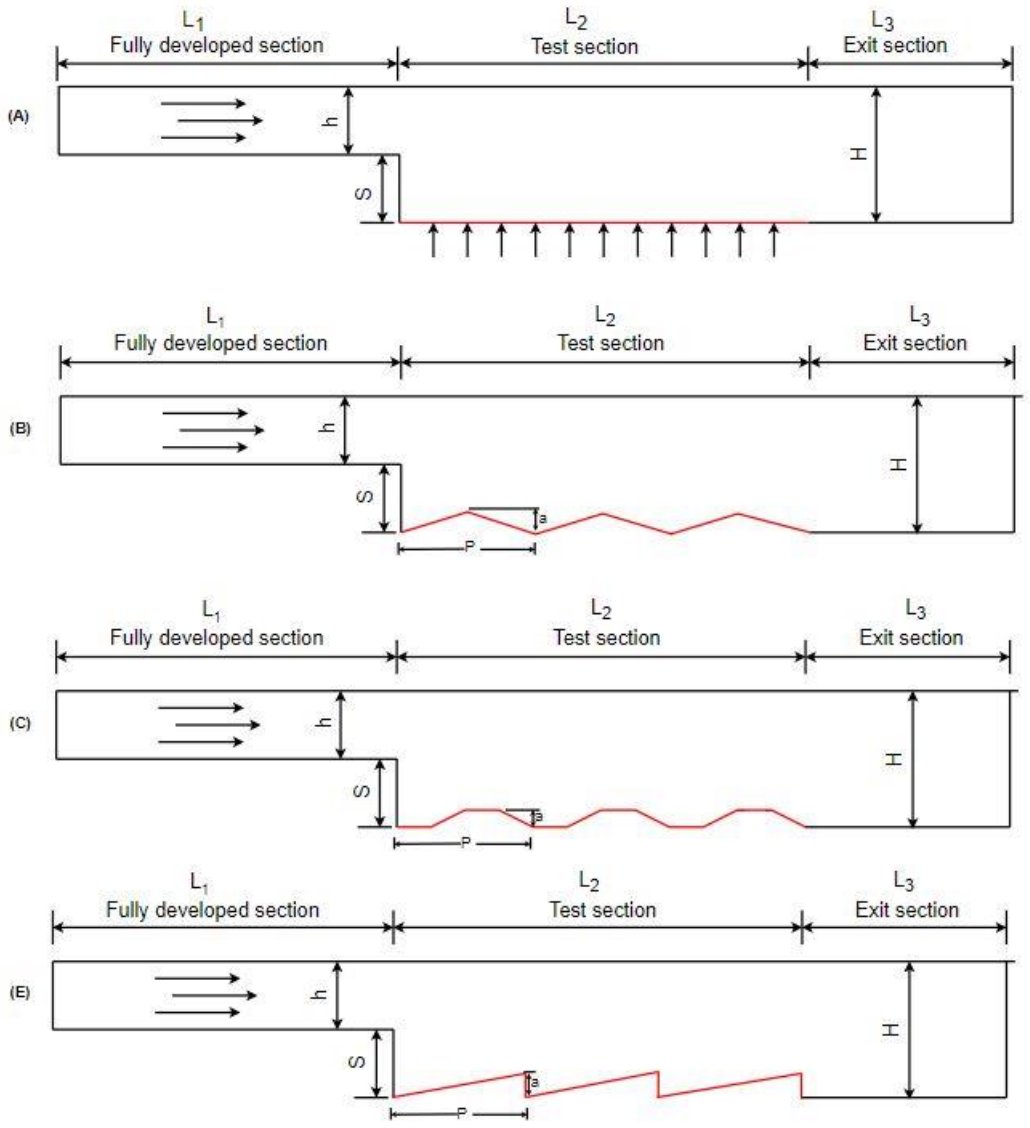

Fig. 1. Schematic diagram of the backward-facing step channels: (A) smooth backward-facing step, (B) backward-facing step with a triangular corrugated bottom, (C) backward-facing step with a trapezoidal corrugated bottom, (E) backward-facing step with zigzag bottom

1.2.2 Governing equations

The governing equations of continuity, momentum, and energy were solved for the turbulent flow under the conditions of steady-state flow, incompressible and Newtonian fluid, two-dimensional, and constant flow. The governing equations were written as follows [36];

The continuity equation:

$$\frac{\partial(\rho\bar{u})}{\partial x}+\frac{\partial(\rho\bar{v})}{\partial y}=0 \tag{1}$$

The x-Momentum equation:

$$\frac{\partial}{\partial x}(\rho\bar{u}\bar{u})+\frac{\partial}{\partial y}(\rho\bar{u}\bar{v})=-\frac{\partial P}{\partial x}+\frac{\partial}{\partial x}\left[(\mu+\mu_t)\frac{\partial\bar{u}}{\partial x}\right]+\frac{\partial}{\partial y}\left[(\mu+\mu_t)\frac{\partial\bar{u}}{\partial y}\right] \tag{2}$$

The y- Momentum equation:

$$\frac{\partial}{\partial x}(\rho\bar{u}\bar{v})+\frac{\partial}{\partial y}(\rho\bar{v}\bar{v})=-\frac{\partial P}{\partial X}+\frac{\partial}{\partial X}\left[(\mu+\mu_t)\frac{\partial\bar{v}}{\partial X}\right]+\frac{\partial}{\partial y}\left[(\mu+\mu_t)\frac{\partial\bar{v}}{\partial y}-\frac{2}{3}\rho\frac{\partial k}{\partial y}\right] \tag{3}$$

The conservation of energy equation:

$$\frac{\partial}{\partial x}(\rho\bar{u}T)+\frac{\partial}{\partial y}(\rho\bar{v}T)=\frac{\partial}{\partial x}\left[\left(\frac{k}{C_P}+\frac{\mu_t}{Pr_t}\right)\frac{\partial T}{\partial x}\right]+\frac{\partial}{\partial y}\left[\left(\frac{k}{C_P}+\frac{\mu_t}{Pr_t}\right)\frac{\partial T}{\partial y}\right] \tag{4}$$

In the above equations μ_t represent the turbulent dynamic viscosity which is related to k and ε, and can be calculated as:

$$\mu_t=\rho C_\mu f_\mu\left(\frac{k^2}{\varepsilon}\right) \tag{5}$$

Using the commercial CFD package of Ansys-Fluent V19, the finite volume method (FVM) was employed to solve the governing equations with corresponding boundary conditions. The SIMPLE algorithm was used to solve the flow field and the second-order upwind differencing scheme was implemented for the convection standings. The $k-\varepsilon$ turbulent model with RNG was selected while the term of diffusion in the momentum and energy equations was approached by the second-order upwind difference. To determine the velocity gradient, the grid was refined near the bottom wall and the step. The scaled residual for energy and velocity components were set at 10^{-9}.

1.2.3 Boundary conditions

The boundary conditions at the inlet section:

$$u = u_{in}, V = 0, T_{in} = 300K, k_{in} = \frac{3}{2}(I\,u_{in})^2, \varepsilon_{in} = C_{\mu}^{\frac{3}{4}} \frac{K^{3/2}}{Lt} \quad (6.0)$$

The fully developed equation [37]:

$$\frac{L}{D} = [(0.631)^{1.6} + 0.0442\,Re)^{1.6}]^{1/1.6} \quad (7.0)$$

The outlet boundary conditions:

$$\frac{\partial k}{\partial x} = \frac{\partial \varepsilon}{\partial x} = 0, \frac{\partial T_f}{\partial x} = 0, and \;\; \frac{\partial u}{\partial x} = \frac{\partial v}{\partial x} = 0 \quad (8.0)$$

The wall:

$$u = V = 0, q = q_{corrugated} \quad (9.0)$$

To determine the flow and heat transfer characteristics in the test channel, the following equation are presented.

The average heat transfer coefficient:

$$h = q\,.\;\frac{\ln\left(\frac{T_w - T_{m,in}}{T_w - T_{m,out}}\right)}{(T_w - T_{m,in}) - (T_w - T_{m,out})} \quad (10.0)$$

$$q = m\,C_p\;(T_w - T_{m,out})/A \quad (11.0)$$

Where A is the corrugated surface area, $T_{m,out}$ and $T_{m,in}$ are the average inlet and outlet temperatures of the working fluid

The inlet velocity:

$$u_{in} = \frac{Re\,\mu}{\rho\,D_h} \quad (12.0)$$

The average Nusselt number:

$$Nu = \frac{hD_h}{k} \quad (13.0)$$

Where D_h is the channel hydraulic diameter which was calculated as follows;

$$D_h = \frac{4A}{p} \quad (14.0)$$

Where P is the channel wetted perimeter and A is the channel cross-sectional area

The friction factor of the channel:

$$f = \frac{2D_h \Delta P}{L\rho u^2} \quad (15.0)$$

Performance evaluation criteria (PEC) was applied to compare the hydraulic and the thermal performance of the channel and PEC was computed as shown below [38].

$$PEC = \frac{(Nu/Nu_o)}{(f/f_0)1/3} \quad (16.0)$$

Where Nu is the Nusselt number and f is the friction factor of the new channel (backward-facing step combined with corrugated wall), while Nu_o is the Nusselt number and f_0 is the friction factor of the original channel (backward-facing step).

1.3 Grid study and code validation

The computational mesh was constructed using the meshing tool in Ansys V.19. A structural mesh based on a rectangular grid was selected in this simulation. To ensure the validity and accuracy of the solution scheme, several grid sizes were examined, namely 69,000; 121,000; 258,000 and 454,000. **Fig.** 2 shows a comparison of *Re* of pure water with $\overline{Nu}$ at four various grids. It was found that the computed results were independent of a number of grid points and the relative error between the second and the third grid was very small and could be neglected to decrease effort and computational time. A grid size of 258,000 was employed. A non-uniform grid was applied in the meshing phase. Finally, there was no change in the average velocity vector, *Nu*, and friction factor when a grid size of 454,000 was applied.

The code was validated by comparing experimental data for fluid flow over backward-facing step channel of Kherbeet *et al*., [39], and corrugated channel of Elshafei *et al*., [40] with numerical predictions. Detailed information of the cases in the code validation is presented in **Table** 2. The validation for the result of the *Nu* and the friction factor for the case of backward-facing step is presented in **Fig.** 3(a-b) and shows a good agreement between the

numerical results of the present study and the results from [39], [40]. Moreover, the average *Nu* for fluid flow in the corrugated channel shows a very close result between the numerical and experimental works as shown in **Fig.** 3(e). The value of y^+ at the bottom wall in the present study was adjusted to the recommended range ≈1, since the enhance wall treatment faction was applied.

Table 2 Details information of the cases in the code validation studies

Case no.	Author	Channel	Flow	Geometry parameters
1	Kherbeet *et al.*, [39]	Backward-facing step	Laminar *Re* = 280	S = 0.6 mm Upstream = 0.1 m Downstream = 0.15 m
2	Elshafei *et al.*, [40]	Corrugated	Turbulent *Re* = 4,000 to 10,000	$\emptyset = 21.8^{\circ}$ Axial length = 100 mm Corrugation pitch = 10 mm

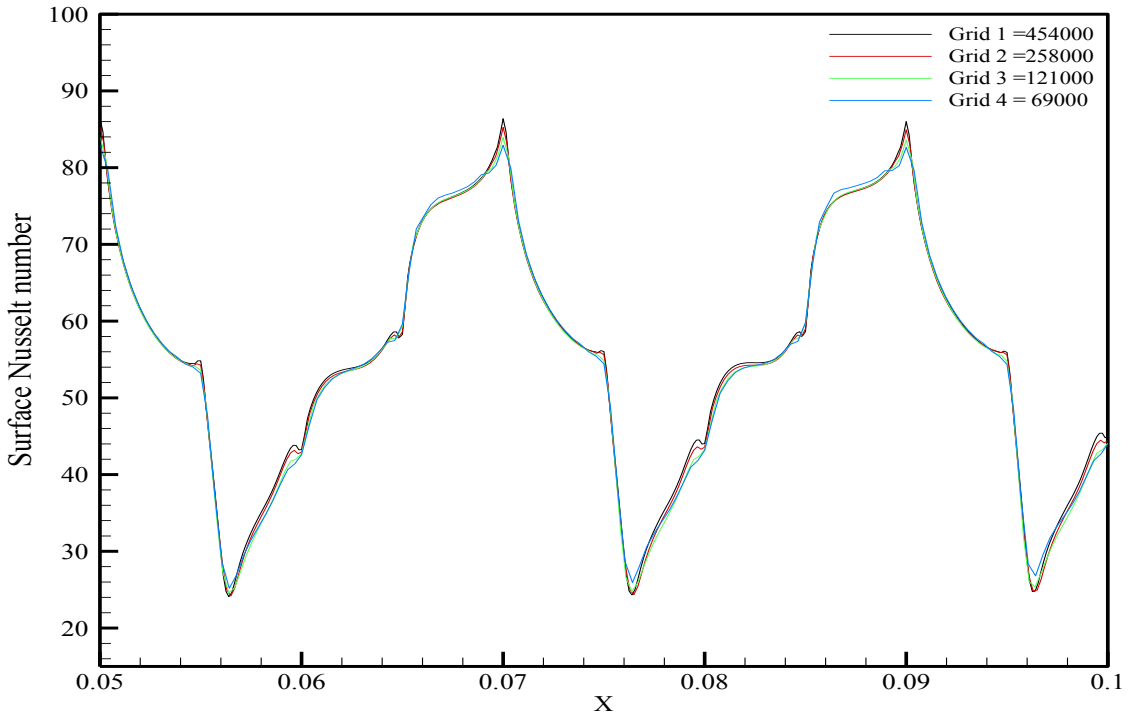

Fig. 2. Grid independent study for the surface Nusselt number $\overline{Nu}$ at *Re* =5,000

(a)

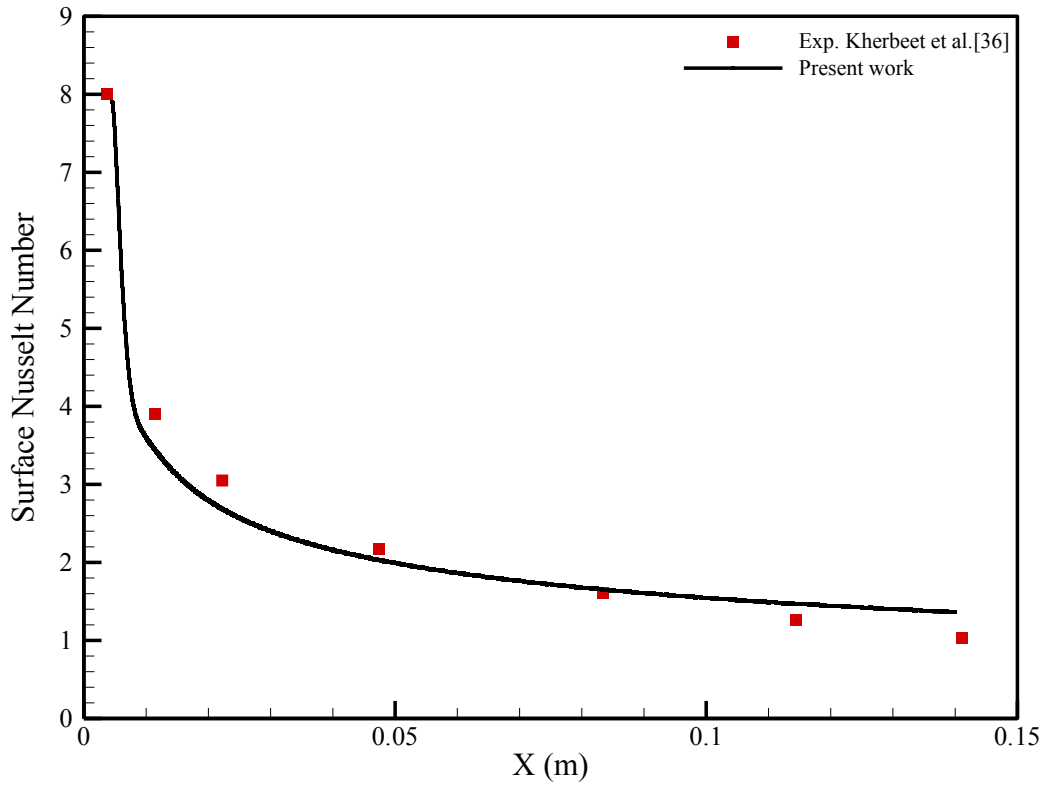
Exp. Kherbeet et al.[36]
Present work
Surface Nusselt Number
X (m)
0
1
2
3
4
5
6
7
8
9
0
0.05
0.1
0.15

(b)

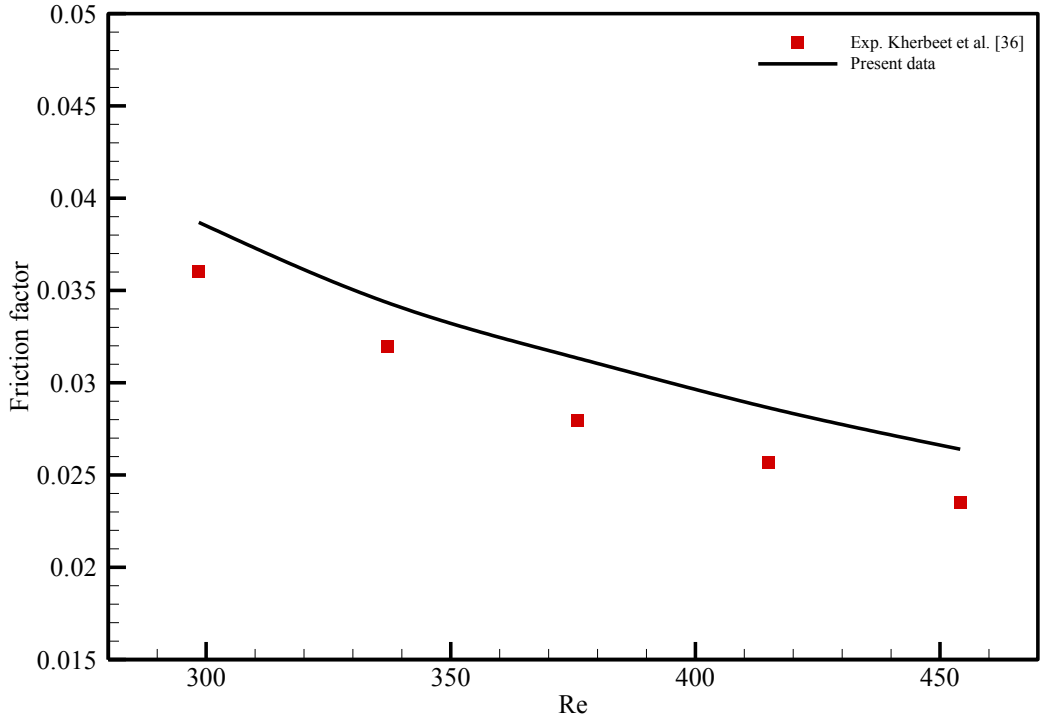
Exp. Kherbeet et al. [36]
Present data
Friction factor
Re
0.05
0.045
0.04
0.035
0.03
0.025
0.02
0.015
300
350
400
450

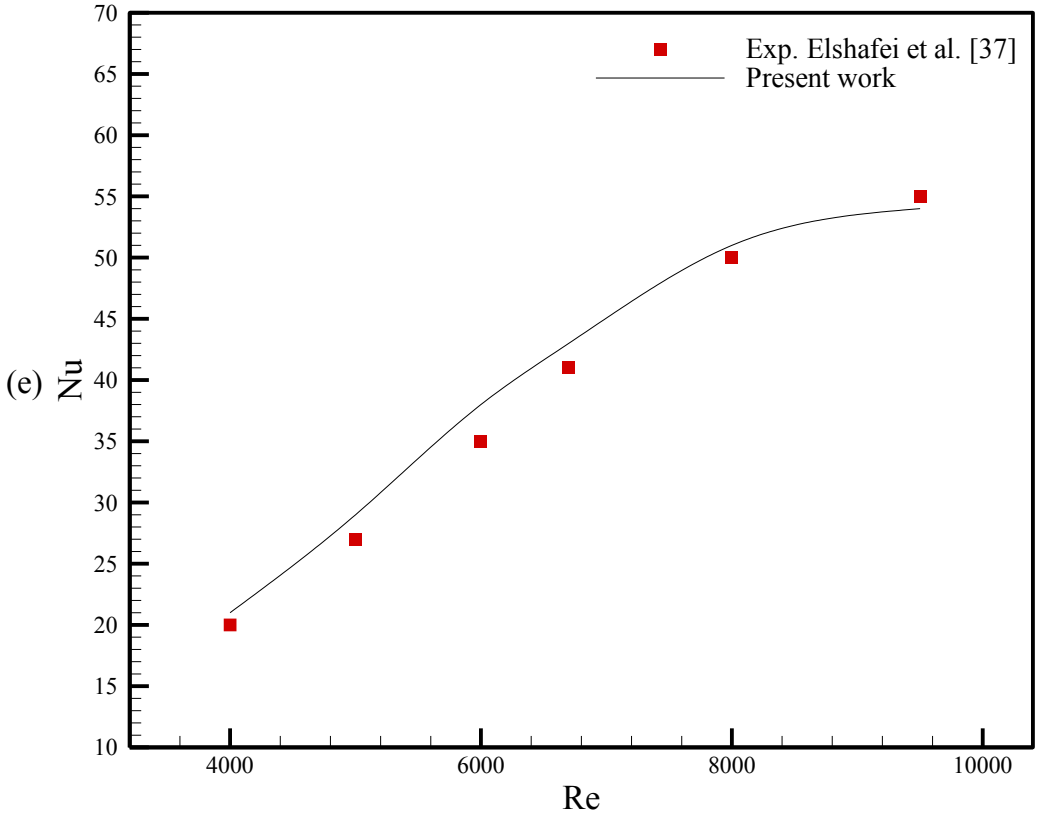

Fig. 3. Validation of the present CFD results for pure water with outcomes from previous studies, (a) $\overline{Nu}$, (b) Friction factor, (e) Average *Nu*

1.4 Results and discussion

The current numerical investigation adopted a backward-facing step with different corrugated walls and constant heat flux. *Re* were in the range of 5,000 to 20,000. The effects of corrugation shape and the *Re* on the thermal and hydraulic performance are presented and interpreted in this section. The results obtained in this study corroborate with previous findings [25], [27], [36], as will be discussed shortly.

1.4.1 Effects of different corrugated shapes

The combination of corrugated wall with backward-facing step showed a significant effect on the fluid flow and heat transfer as demonstrated in **Fig.** 4(A, B) which presents the $\overline{Nu}$ and the skin friction coefficient along the corrugated wall for each channel at *Re* = 5,000, pitch

diameter = 20 mm and amplitude height = 4 mm. It was observed that the $\overline{Nu}$ for the trapezoidal corrugated bottom was the highest compared to the other shapes and the straight bottom had the lowest $\overline{Nu}$. In contrast, the skin friction coefficient for the straight bottom shows the lowest value followed by zigzag, trapezoidal and triangular corrugated respectively. **Fig.** 4(B) shows that the distributions of skin friction coefficient of all corrugated walls have a different frequency as that of the corrugated surface, and the highest and lowest values occur precisely at the location of the lowest and highest cross-section of the corrugation surface. The heat transfer enhancement was associated with the trouble of flow and the flow over the trapezoidal corrugated bottom created a higher recirculation region and thin boundary layer. This implies that the trapezoidal corrugated bottom was more effective with backward-facing step and gave better $\overline{Nu}$ rates. Moreover, **Fig.** 4(A) shows that the $\overline{Nu}$ is higher in the converging section of each wave of the corrugation shape than in the diverging section. This is because the velocity gradient and the average velocity of the converging section are higher, and that leads to an increase in the heat transfer ratio. The $\overline{Nu}$ is almost constant after the third corrugation of each channel, i.e. as soon as the flow becomes fully developed.

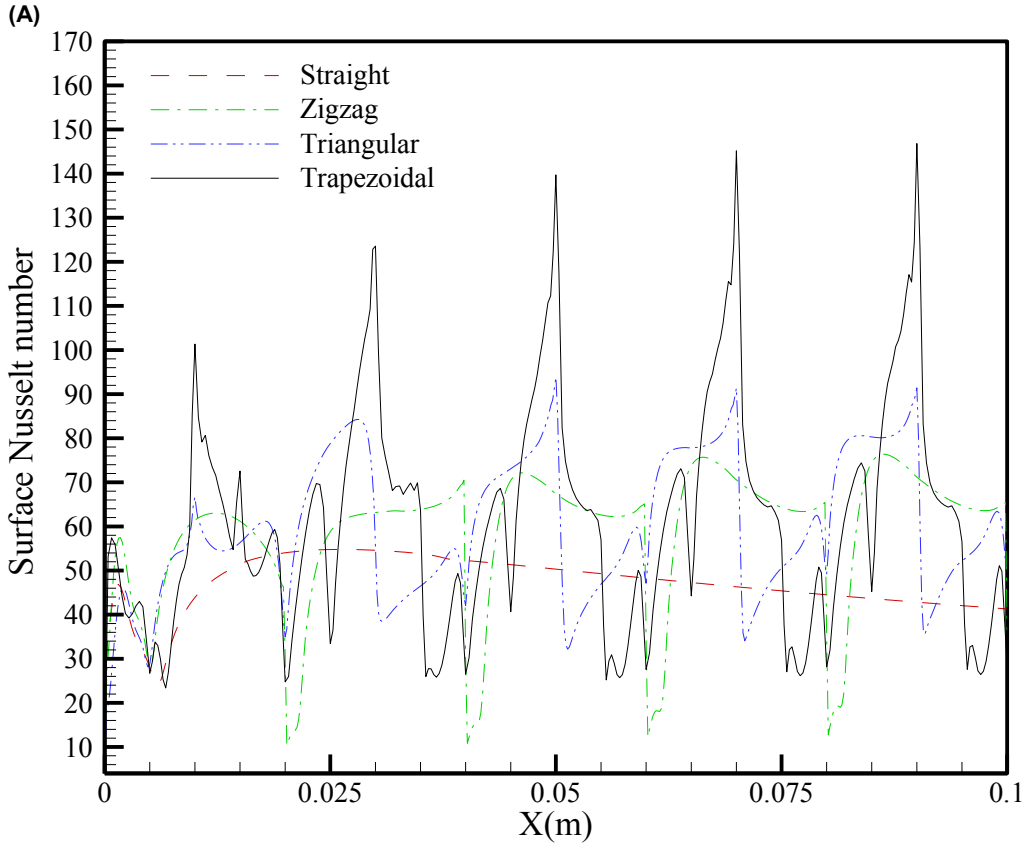
(A)
Straight
Zigzag
Triangular
Trapezoidal
Surface Nusselt number
X(m)
170
160
150
140
130
120
110
100
90
80
70
60
50
40
30
20
10
0
0.025
0.05
0.075
0.1

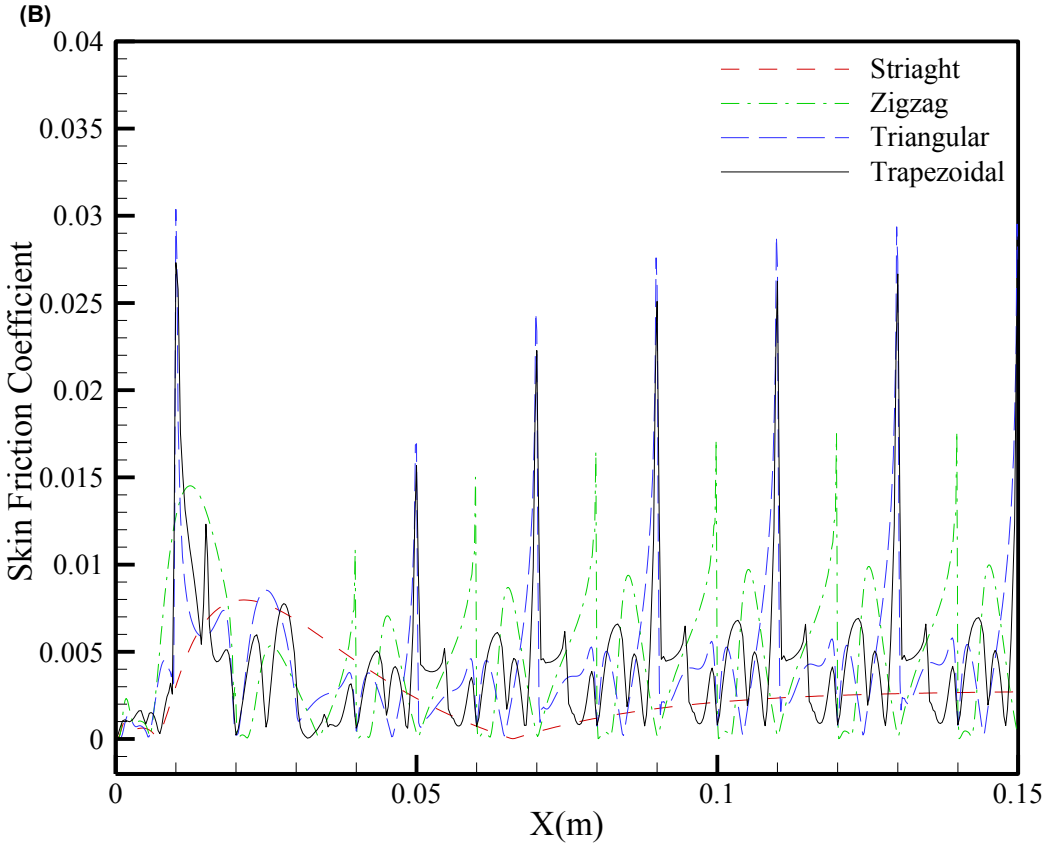

Fig. 4. The distribution of (A) $\overline{Nu}$ and (b) Skin friction coefficient along the axial direction of the channel at *Re* = 5,000

The results of the average *Nu* with *Re* for the different corrugated shapes are presented in **Fig.** 5. The four cases show the same pattern where the *Nu* increased with the flow rate. This is because the strong turbulence intensity of the corrugated wall generates a hasty mixing between the core and the wall of the channel. The trapezoidal corrugated bottom has the highest improvement of heat transfer compared to the other designs. This could be because of the strong recirculation regime size formed between the corrugated carves which was bigger than the other designs, leading to an increased temperature gradient.

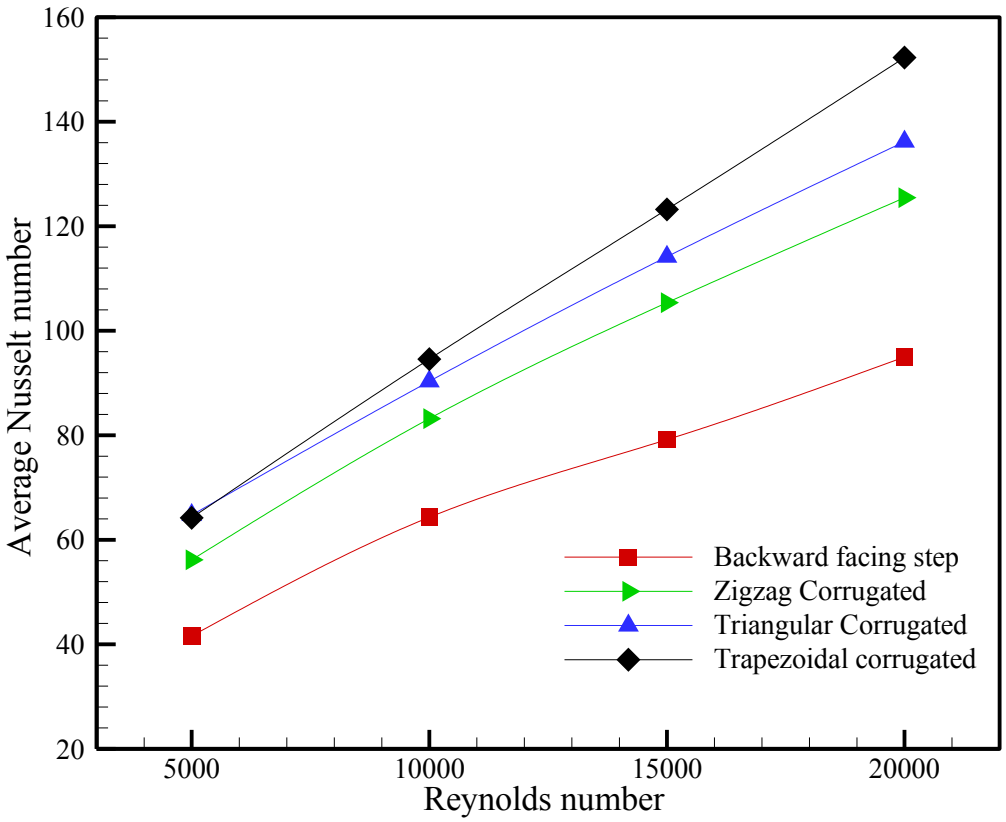

Fig. 5. Average *Nu* for various channels with different *Re*

Fig. 6 shows the skin friction coefficient with *Re* along the channels. It should be noted that the *Re* increased from 5,000 to 20,000, the overall trend shows that skin friction was higher at *Re* = 5,000 and decrease with an increase of *Re* since the average skin friction is inversely proportional to the velocity. The backward-facing step with the triangular corrugated showed the highest average skin friction compared with the smooth backward-facing step, while the trapezoidal and zigzag corrugated gave almost the same value.

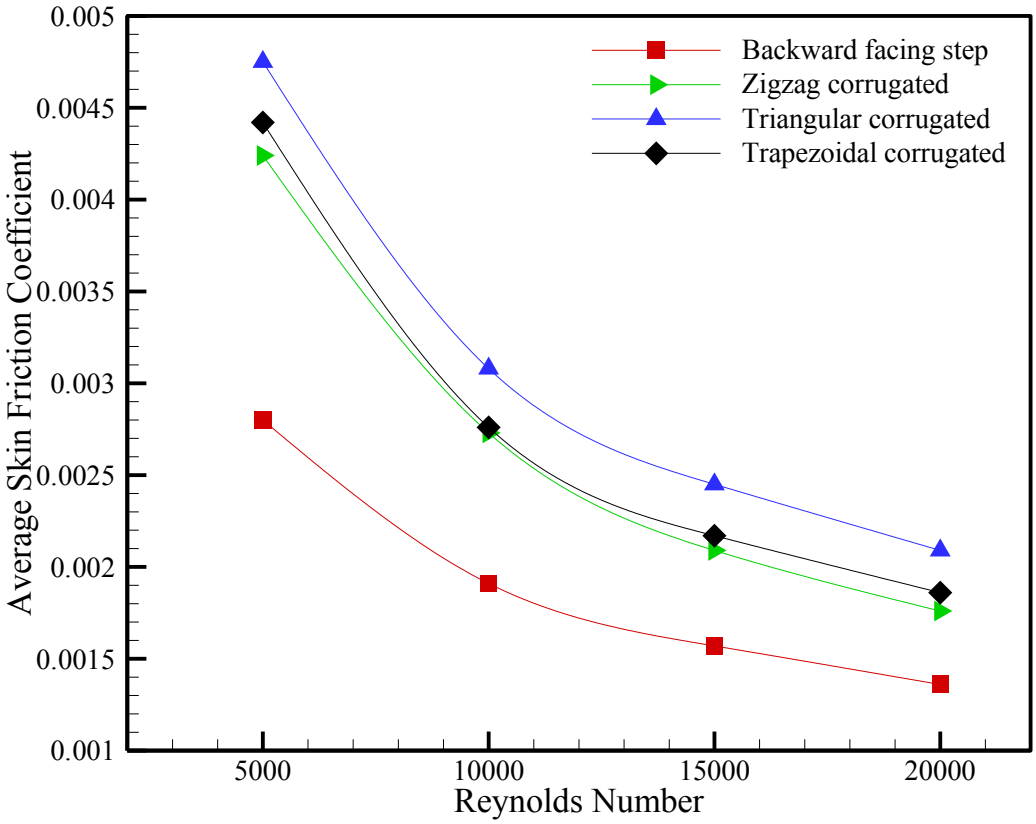

Fig. 6. Skin friction factor for various channels with different *Re*

The effects of different amplitude heights on surface Nusselt number at pitch diameter = 20 mm and *Re* = 5,000 are plotted in **Fig.** 7(A). The same trend is observed for all values of amplitude height tested in this investigation. The increase of amplitude height had an important effect on $\overline{Nu}$ augmentation. This could be due to the high velocity gradient at the trapezoidal corrugated surface, which was increasing as the amplitude height increased. The value of $\overline{Nu}$ at an amplitude height of 4 mm was almost double the value at an amplitude height of 1 mm. However, there is no significant increment after the amplitude height of 4 mm and that could be because of the constant of distribution in the average velocity and the velocity gradient.

Fig. 7(B) presents the distribution of the local skin friction coefficient for different amplitude heights (1, 2, 3, 4, and 5 mm), where *Re* = 5,000 through backward-facing step with trapezoidal corrugation. It shows that the value of skin friction increases as the amplitude height increases, and that is due to the increase in the pressure in the channel where

increasing the amplitude height leads to reduce the cross-section area. Moreover, the maximum and minimum value occur precisely at the highest and lowest value of the amplitude height.

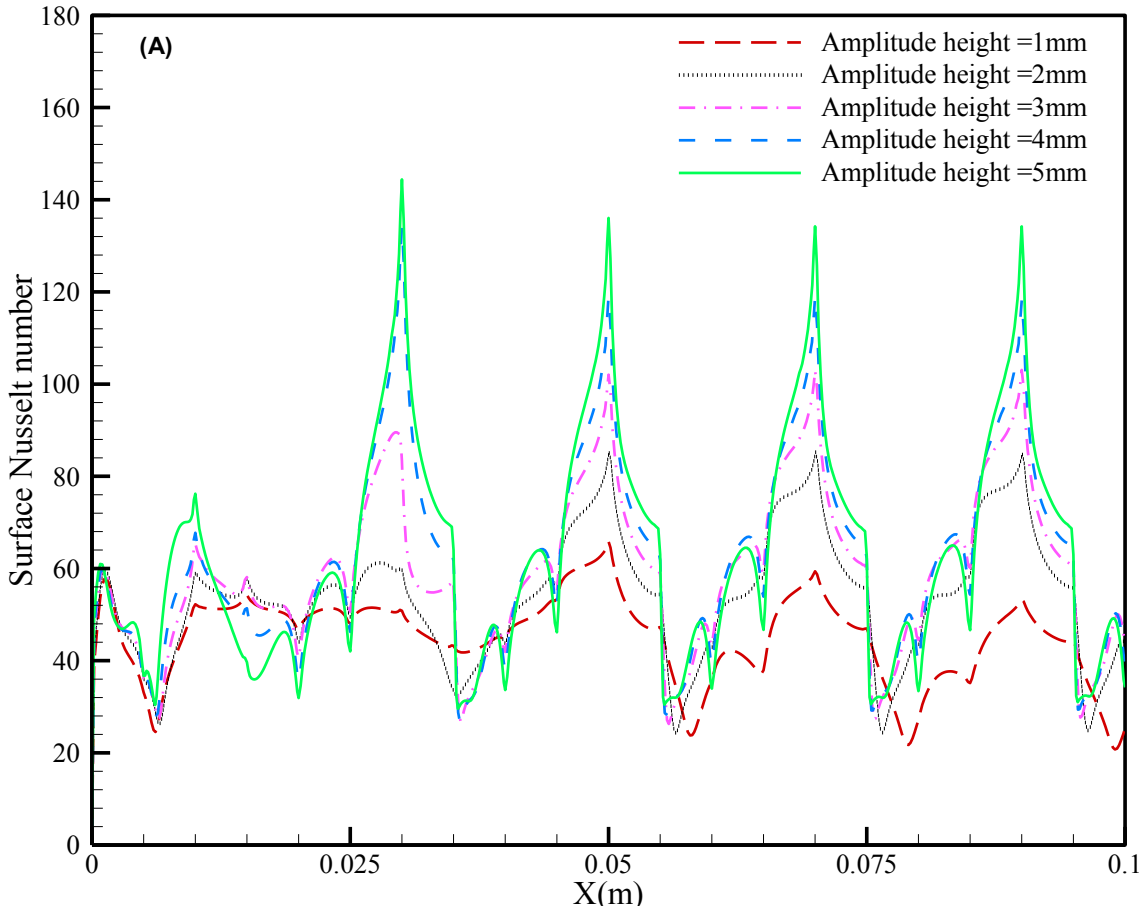

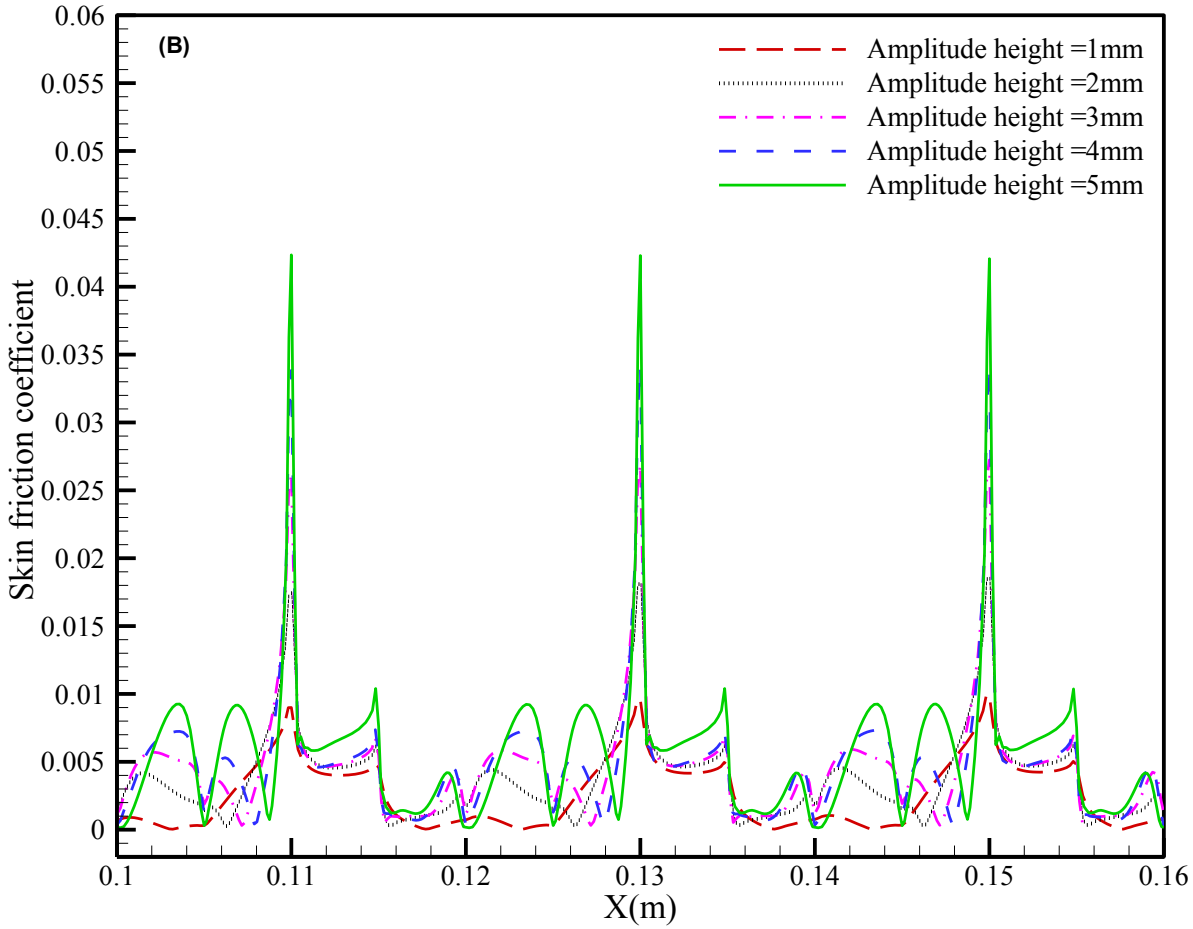

Fig. 7. The effect of amplified height on (A) surface Nusselt number and (B) skin friction coefficient at *Re* = 5,000 through trapezoidal corrugated

1.4.2 Fluid flow and velocity streamline

The effects of different corrugated shapes on the velocity distribution at *Re* = 5,000, pitch diameter of 20 mm and amplitude height of 4 mm is illustrated in **Fig.** 8. As can be observed from the figure, the recirculation region was formed next to the corner of a step, which is in line with the result of fluid flow over backward-facing step channel reported in previous literature [5], [11], [13], [41], [42]. The converging and diverging section of corrugated walls played an important role in the velocity streamline. A stable secondary vortex was formed at the diverging section of the corrugated wall of each shape due to the wrinkle sharp edge of the corrugated wall. Corrugation also breaks the main recirculation of the flow just after the backward facing step, reducing the length of this main recirculation (e.g. compare Figure 8a with Figures 8b, 8c or 8d). The maximum velocity gradient behind the step observed at the

backward-facing step with the trapezoidal corrugated wall as shown in **Fig.** 8d. This increment in the velocity gradient leads to a thinner thermal boundary layer at the converging section of the trapezoidal corrugated wall. The velocity streamlines near the walls are always low due to the friction between the viscous sublayers and the wall. However, using the corrugation walls in backward-facing step channel increases velocity distribution near the wall and this leads to better mixing of the flow layers.

1.4.3 Performance evaluation criteria

The increment in the pressure drop was associated with the heat transfer augmentation. Therefore, it is very important to evaluate the efficiency of utilising a corrugated wall by using PEC. Higher values of PEC led to higher heat transfer rate. Moreover, a PEC value of more than 1 implied that the heat transfer rate was greater than the rise in the pressure drop [38]. The effect of *Re* on PEC, at different amplitude heights is illustrated in **Fig.** 9. The value of PEC increased with the increase of amplitude height because PEC is a factor of *Nu* and friction. However, the maximum increment occurred at the amplitude height of 4 mm and decreased at the amplitude height of 5 mm due to the incensement of friction factor and the limited increase of *Nu*.

Fig. 10 shows the effect of *Re* on performance evaluation criteria for triangular, trapezoidal and zigzag corrugated shape. The value of the PEC for trapezoidal was higher compared to the other shapes due to the significant enhancement in heat transfer through that channel. Moreover, the PEC increased with an increment of *Re*.

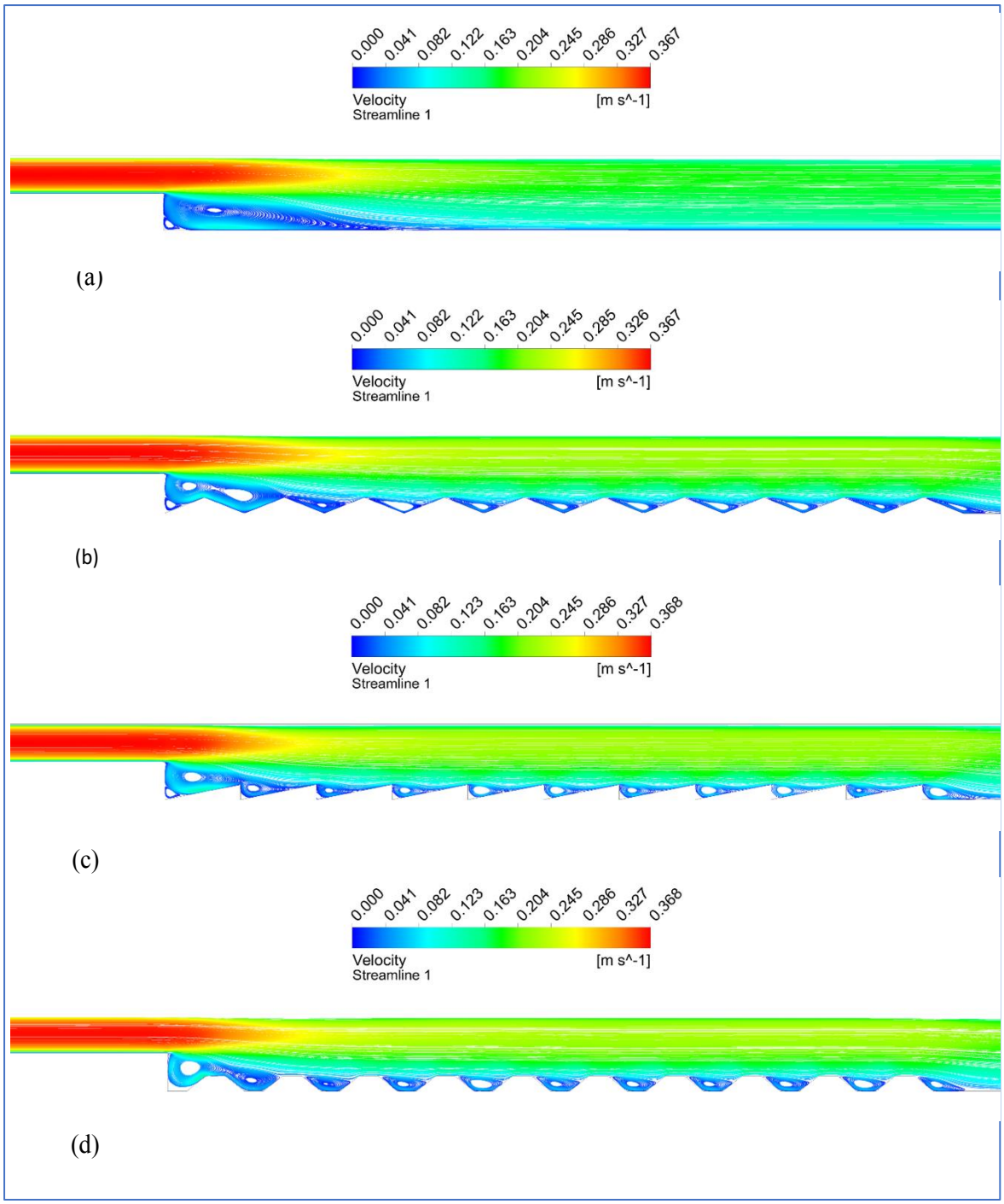

Fig. 8. Velocity streamlines through backward-facing step with (a) straight bottom, (b) triangular bottom, (c) zigzag bottom, and (d) trapezoidal bottom

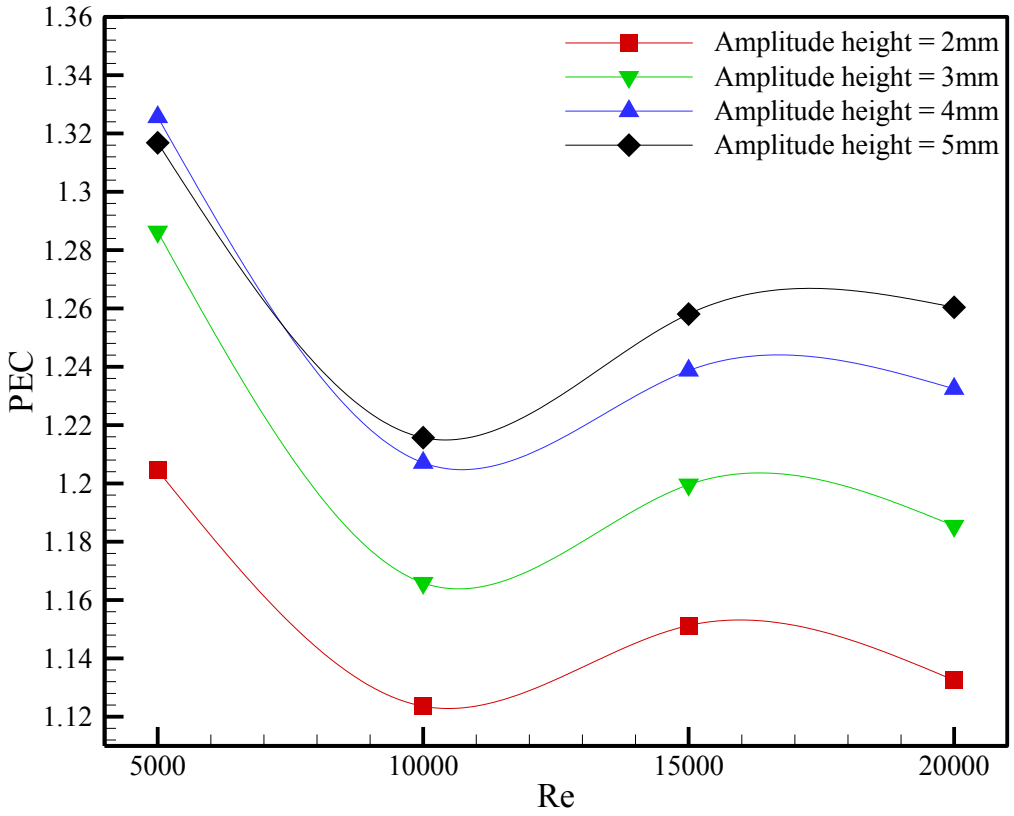

Fig. 9. PEC with *Re* for different amplitude heights

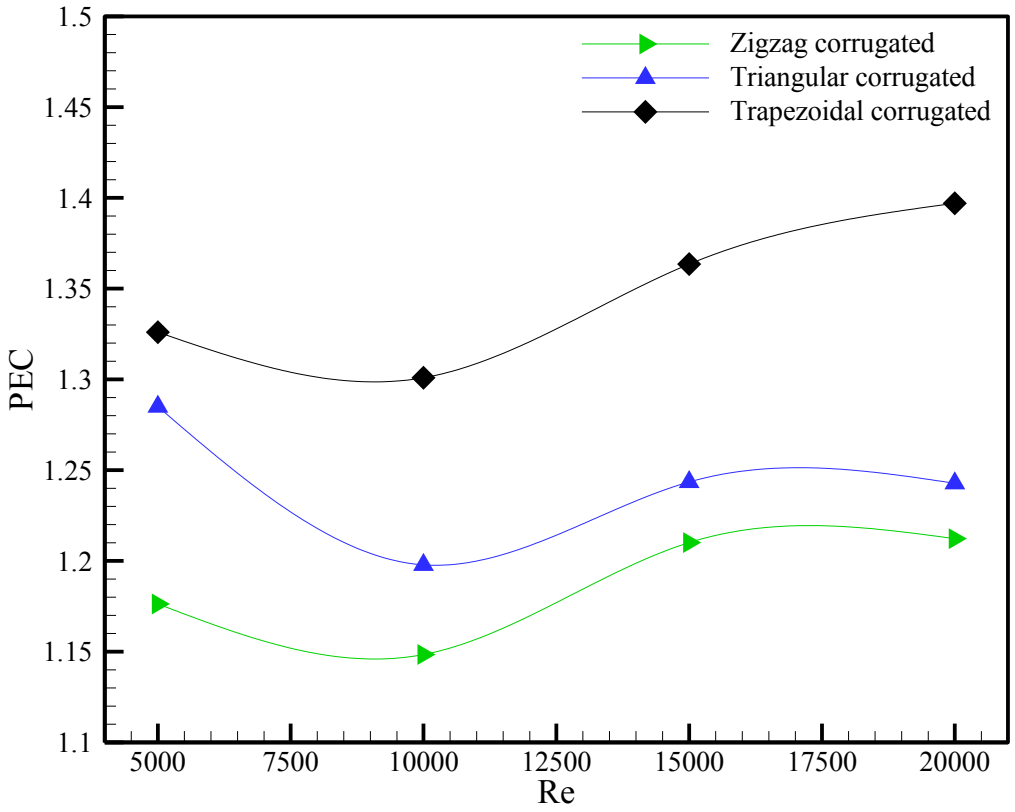

Fig. 10. PEC with *Re* for different corrugated shapes

1.5 Conclusion

A set of CFD simulation of turbulent flow over backward-facing step with a different corrugated bottom was conducted, analysed and discussed. The effects of corrugated design on the heat transfer enhancement under constant heat flux were investigated. The pitch diameter of the corrugated wall was kept constant. The main objective focused on the heat transfer enhancement that occurred from different parameters, such as corrugated shape (trapezoidal, triangular and zigzag), amplitude height and *Re*.

The present results showed that the corrugated bottom wall enhanced the heat transfer over the backward-facing step channel. It was observed that the trapezoidal shape obtained the higher performance evaluation criteria (PEC = 1.326), which is a factor of *Nu* and friction. Furthermore, the amplitude height had a significant effect on the heat transfer enhancement,

where higher amplitude led to greater heat transfer rate. Finally, the velocity distribution and *Nu* increased progressively as the *Re* increased and skin friction coefficient decreased.

It can be concluded that the best improvement in the heat transfer rate over the backward-facing step could be obtained by using a trapezoidal corrugated bottom with an amplitude height of 4 mm at *Re* = 5,000. The laminar flow over these channels and different corrugated dimensions may be considered for future work.

Acknowledgment

The authors are grateful to University Putra Malaysia for providing the necessary equipment for this research and their generous support through the International Graduate Scholarship (IGSS).

References

[1] W. A. Xie and G. N. Xi, "Geometry effect on flow fluctuation and heat transfer in unsteady forced convection over backward and forward facing steps," *Energy*, vol. 132, pp. 49–56, 2017.

[2] A. Hilo, A. Rahim, A. Talib, S. R. Nfawa, M. Thariq, and H. Sultan, "Review of improvements on heat transfer using nanofluids via corrugated facing step," *IJET*, vol. 7, no. (4.13), pp. 160–169, 2018.

[3] Y. T. Chen, "Turbulent separated convection flow adjacent to backward-facing step — effects of step height," *Int. J. Heat Mass Transf.*, vol. 49, pp. 3670–3680, 2006.

[4] A. Ebrahimi, F. Rikhtegar, A. Sabaghan, and E. Roohi, "Heat transfer and entropy generation in a microchannel with longitudinal vortex generators using nano fl uids," *Energy*, vol. 101, pp. 190–201, 2016.

[5] H. I. Abu-Mulaweh, B. F. Armaly, and T. S. Chen, "Measurements in buoyancy-assisting laminar boundary layer flow over a vertical backward-facing step-Uniform wall heat flux case," *Exp. Therm. Fluid Sci.*, vol. 7, no. 1, pp. 39–48, 1993.

[6] J. T. Lin, B. F. Armalyy, and T. S. Chen, "Mixed convection heat transfer in inclined backward-facing step flows," *Int. J. Heat Mass Transf.*, vol. 34, no. 6, pp. 1568–1571, 1991.

[7] G. C. Vradis and L. Vannostrandt, "Laminar Coupled Flow Downstream of an Asymmetric Sudden Expansion," *J. Thermophys. Heat Transf.*, vol. 6, no. 2, pp. 288–295, 1992.

[8] H. Iwai, K. Nakabe, and K. Suzuki, "Flow and heat transfer characteristics of backward-facing step laminar flow in a rectangular duct," *Int. J. Heat Mass Transf.*, vol. 43, pp. 457–471, 2000.

[9] T. S. S. Chen, B. F. F. Armaly, H. I. Abu-Mulaweh, T. S. S. Chen, and B. F. F. Armaly, "Turbulent mixed convection flow over a backward-facing step—the effect of the step heights," *Int. J. Heat Fluid Flow*, vol. 23, no. 6, pp. 758–765, 2002.

[10] M. Bahiraei and M. Hangi, "Numerical simulation of nano fl uid application in a C-shaped chaotic channel : A potential approach for energy ef fi ciency improvement," *Energy*, vol. 74, pp. 863–870, 2014.

[11] E. Abu-Nada, "Entropy generation due to heat and fluid flow in backward facing step flow with various expansion ratios," *Int. J. Exergy*, vol. 3, no. 4, p. 419, 2006.

[12] J. H. Nie and B. F. Armaly, "Three-dimensional convective flow adjacent to backward-facing step - effects of step height," *Int. J. Heat Mass Transf.*, vol. 45, pp. 2431–2438, 2002.

[13] B. F. Armaly, A. Li, and J. H. Nie, "Measurements in three-dimensional laminar separated flow," *Int. J. Heat Mass Transf.*, vol. 46, no. 19, pp. 3573–3582, 2003.

[14] A. A. Al-aswadi, H. A. Mohammed, N. H. Shuaib, and A. Campo, "Laminar forced convection flow over a backward facing step using nanofluids," *Int. Commun. Heat Mass Transf.*, vol. 37, no. 8, pp. 950–957, 2010.

[15] H. Togun *et al.*, "Numerical simulation of laminar to turbulent nanofluid flow and heat transfer over a backward-facing step," *Appl. Math. Comput.*, vol. 239, pp. 153–170, 2014.

[16] H. Xue and S. Chen, "Dsmc simulation of microscale backward-facing step flow," *Microscale Thermophys. Eng.*, vol. 7, no. 1, pp. 69–86, 2003.

[17] H. Xue, B. Xu, Y. Wei, and J. Wu, "Unique behaviors of a backward-facing step flow at microscale," *Numer. Heat Transf. Part A Appl.*, vol. 47, no. 3, pp. 251–268, 2005.

[18] T. Y. Hsieh, Z. C. Hong, and Y. C. Pan, “Flow characteristics of three-dimensional microscale backward-facing step flows,” *Numer. Heat Transf. Part A Appl.*, vol. 57, no. 5, pp. 331–345, 2010.

[19] H. A. Mohammed, A. A. Al-Aswadi, N. H. Shuaib, and R. Saidur, “Convective heat transfer and fluid flow study over a step using nanofluids: A review,” *Renew. Sustain. Energy Rev.*, vol. 15, no. 6, pp. 2921–2939, 2011.

[20] F. Selimefendigil and H. F. Öztop, “Forced convection and thermal predictions of pulsating nanofluid flow over a backward facing step with a corrugated bottom wall,” *Int. J. Heat Mass Transf.*, vol. 110, pp. 231–247, 2017.

[21] S. Singh, B. Singh, V. S. Hans, and R. S. Gill, “CFD (computational fl uid dynamics) investigation on Nusselt number and friction factor of solar air heater duct roughened with non-uniform cross-section transverse rib,” *Energy*, vol. 84, pp. 509–517, 2015.

[22] F. Bozzoli, L. Cattani, and S. Rainieri, “Effect of wall corrugation on local convective heat transfer in coiled tubes,” *Int. J. Heat Mass Transf.*, vol. 101, pp. 76–90, 2016.

[23] M. Mirzaei, L. Davidson, A. Sohankar, and F. Innings, “The effect of corrugation on heat transfer and pressure drop in channel flow with different Prandtl numbers,” *Int. J. Heat Mass Transf.*, vol. 66, pp. 164–176, 2013.

[24] H. A. Mohammed, A. M. Abed, and M. A. Wahid, “The effects of geometrical parameters of a corrugated channel with in out-of-phase arrangement,” *Int. Commun. Heat Mass Transf.*, vol. 40, no. 1, pp. 47–57, 2013.

[25] M. A. Sheremet, I. Pop, and N. C. Roşca, “Magnetic field effect on the unsteady natural convection in a wavy-walled cavity filled with a nanofluid: Buongiorno’s mathematical model,” *J. Taiwan Inst. Chem. Eng.*, vol. 61, pp. 211–222, 2016.

[26] S. D. Pandey and V. K. Nema, “Experimental analysis of heat transfer and friction factor of nanofluid as a coolant in a corrugated plate heat exchanger,” *Exp. Therm. Fluid Sci.*, vol. 38, pp. 248–256, 2012.

[27] K. Schmidmayer, P. Kumar, P. Lavieille, and M. Miscevic, “Thermo-hydraulic characterization of a self-pumping corrugated wall heat exchanger,” vol. 128, pp. 713–728, 2017.

[28] R. K. Ajeel, W. S. I. W. Salim, and K. Hasnan, “Thermal and hydraulic characteristics of turbulent nanofluids flow in trapezoidal-corrugated channel: Symmetry and zigzag shaped,” *Case Stud. Therm. Eng.*, vol. 12, no. March, pp. 620–635, 2018.

[29] A. M. Abed, M. A. Alghoul, K. Sopian, H. A. Mohammed, H. sh Majdi, and A. N. Al-Shamani, “Design characteristics of corrugated trapezoidal plate heat exchangers using nanofluids,” *Chem. Eng. Process. Process Intensif.*, vol. 87, pp. 88–103, 2015.

[30] M. A. Ahmed, M. Z. Yusoff, K. C. Ng, and N. H. Shuaib, “Numerical and experimental investigations on the heat transfer enhancement in corrugated channels using SiO2–water nanofluid,” *Case Stud. Therm. Eng.*, vol. 6, pp. 77–92, 2015.

[31] A. S. Navaei, H. A. Mohammed, K. M. Munisamy, H. Yarmand, and S. Gharehkhani, “Heat transfer enhancement of turbulent nanofluid flow over various types of internally corrugated channels,” *Powder Technol.*, vol. 286, pp. 332–341, 2015.

[32] S. Eiamsa-ard and P. Promvonge, “Numerical study on heat transfer of turbulent channel flow over periodic grooves,” *Int. Commun. Heat Mass Transf.*, vol. 35, no. 7, pp. 844–852, 2008.

[33] R. K. Ajeel, W. S. W. Salim, and K. Hasnan, “Influences of geometrical parameters on the heat transfer characteristics through symmetry trapezoidal-corrugated channel using SiO2 -

water nanofluid," *Int. Commun. Heat Mass Transf.*, vol. 101, no. January, pp. 1–9, 2019.

[34] H. A. Mohammed, F. Fathinia, H. B. Vuthaluru, and S. Liu, "CFD based investigations on the effects of blockage shapes on transient mixed convective nano fl uid fl ow over a backward facing step," *Powder Technol.*, vol. 346, pp. 441–451, 2019.

[35] H. E. Ahmed, A. S. Kherbeet, M. I. Ahmed, and B. H. Salman, "Heat transfer enhancement of micro-scale backward-facing step channel by using turbulators," *Int. J. Heat Mass Transf.*, vol. 126, pp. 963–973, 2018.

[36] S. A. M. Said, M. A. Habib, H. M. Badr, and S. Anwar, "Turbulent natural convection between inclined isothermal plates," *Comput. Fluids*, vol. 34, no. 9, pp. 1025–1039, 2005.

[37] F. Durst, S. Ray, B. Ünsal, and O. A. Bayoumi, "The Development Lengths of Laminar Pipe and Channel Flows," *J. Fluids Eng.*, vol. 127, no. 6, p. 1154, 2005.

[38] O. Manca, S. Nardini, and D. Ricci, "A numerical study of nanofluid forced convection in ribbed channels," *Appl. Therm. Eng.*, vol. 37, pp. 280–292, 2012.

[39] A. S. Kherbeet, H. A. Mohammed, B. H. Salman, H. E. Ahmed, and O. A. Alawi, "Experimental and numerical study of nanofluid flow and heat transfer over microscale backward-facing step," *Int. J. Heat Mass Transf.*, vol. 79, pp. 858–867, 2014.

[40] E. A. M. Elshafei, M. M. Awad, E. El-Negiry, and A. G. Ali, "Heat transfer and pressure drop in corrugated channels," *Energy*, vol. 35, no. 1, pp. 101–110, 2009.

[41] C. Y. Soong and W. C. Hsueh, "Mixed convection in a suddenly-expanded channel with effects of cold fluid injection," *Int. J. Heat Transf.*, vol. 36, no. 6, pp. 1477–1484, 1993.

[42] M. P. Boruah, P. R. Randive, and S. Pati, "International Journal of Heat and Mass Transfer Hydrothermal performance and entropy generation analysis for mixed convective flows over a backward facing step channel with baffle," *Int. J. Heat Mass Transf.*, vol. 125, pp. 525–542, 2018.